

# Natural Attenuation Potential of Vinyl Chloride and Butyl Acrylate Released in the East Palestine, Ohio Train Derailment Accident

Gao Chen, Sam Rosolina, Elizabeth Padilla-Crespo, Guang He, Qiao Chen, Ana Arosemena, Bryan E. Rosado-Maldonado, Cynthia M. Swift, Paula Belmont Coelho, Andrew J. Whelton, Dora Taggart, and Frank E. Löffler\*



Cite This: *Environ. Sci. Technol.* 2024, 58, 17743–17755



Read Online

ACCESS |

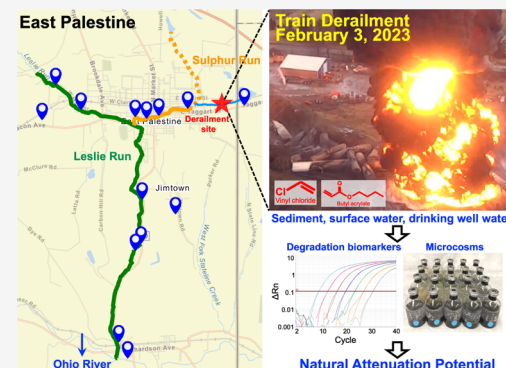
Metrics & More

Article Recommendations

SI Supporting Information

**ABSTRACT:** The East Palestine, Ohio train derailment released toxic vinyl chloride (VC) and butyl acrylate (BA), which entered the watershed. Streambed sediment, surface water, and private well water samples were collected 128 and 276 days postaccident to assess the natural attenuation potential of VC and BA by quantifying biodegradation biomarker genes and conducting microcosm treatability studies. qPCR detected the aerobic VC degradation biomarkers *etnC* in ~40% and *etnE* in ~27% of sediments collected in both sampling campaigns in abundances reaching  $10^5$  gene copies  $g^{-1}$ . The 16S rRNA genes of organohalide-respiring *Dehalococcoides* and *Dehalogenimonas* were, respectively, detected in 50 and 64% of sediment samples collected 128 days postaccident and in 63 and 88% of sediment samples collected 276 days postaccident, in abundances reaching  $10^7$  cells  $g^{-1}$ . Elevated detection frequencies of VC degradation biomarker genes were measured immediately downstream of the accident site (i.e., Sulphur Run). Aerobic VC degradation occurred in all sediment microcosms and coincided with increases of *etnC/etnE* genes and *Mycobacterium*, a genus comprising aerobic VC degraders. The conversion of VC to ethene and an increased abundance of VC reductive dechlorination biomarker genes were observed in microcosms established with sediments collected from Sulphur Run. All anoxic microcosms rapidly degraded BA to innocuous products with intermediate formation of *n*-butanol and acrylate. The results indicate that microbiomes in the East Palestine watershed have natural attenuation capacity for VC and BA. Recommendations are made to improve first-response actions in future contaminant release accidents of this magnitude.

**KEYWORDS:** East Palestine, train derailment, accidental toxin release, vinyl chloride, butyl acrylate, microcosms, molecular biological tools, natural attenuation



## INTRODUCTION

To meet societal demands for common products, precursor materials must be transported to production facilities, with trains playing a major role to meet the logistical challenges. Freight trains carry hazardous materials over long distances, and the United States witnessed more than 1,164 train derailments in 2022 (i.e., ~three derailments day<sup>-1</sup>).<sup>1</sup> On February 3, 2023, a 150-car Norfolk Southern train derailed near the village of East Palestine, OH. Among the 38 derailed cars, four were loaded with polyvinyl chloride (PVC), and 11 carried flammable and hazardous materials, including five tank cars with vinyl chloride (VC) and one with butyl acrylate (BA) (Table S1). Leakage of hazardous materials as well as an ensuing fire required authorities to quickly decide on risk mitigation strategies. VC is transported as a liquefied compressed gas, but the pressure relief valves on at least some of the derailed VC tank cars malfunctioned. Concerns were raised regarding the polymerization of the stabilized VC, which could have led to an explosion. Three days after the accident, a decision was made to puncture the high-risk cars

and drain ~450 tons (t) of VC and ~113 t of BA into a makeshift pit for a “controlled burn”.<sup>2–4</sup> The burn unleashed an extensive smoke plume loaded with particulates.<sup>5</sup> The distribution and impact of combustion byproducts, including polychlorinated dibenzodioxins (PCDDs) and polychlorinated dibenzofurans (PCDFs), remain under investigation. This study explores potential attenuation of VC and BA, both toxic chemicals that were directly released in the accident and penetrated the soil and vadose zone, leading to surface and groundwater contamination.<sup>6,7</sup> The primary surface water body impacted was Sulphur Run, a small tributary to Leslie Run whose waters eventually drain via Little Beaver Creek into the

Received: May 8, 2024

Revised: September 17, 2024

Accepted: September 18, 2024

Published: September 30, 2024



Ohio River, which supplies drinking water to millions of people.

VC is acutely toxic causing eye, mucous membrane, and respiratory tract irritation and classified as a group A human carcinogen.<sup>8,9</sup> The U.S. Environmental Protection Agency (EPA) enforces a drinking water maximum contaminant level (MCL) of 2 ppb VC and recommends an MCL goal for all drinking water of 0 ppb.<sup>10</sup> Hence, controlling VC exposure has been a primary concern following the East Palestine train derailment. VC is mainly used to produce PVC, a widely used plastic.<sup>11</sup> VC is susceptible to biodegradation, and different microbial processes contribute to the transformation and detoxification of VC. In the presence of oxygen (O<sub>2</sub>), VC can serve as a carbon and energy source for taxonomically diverse etheneotrophs (i.e., ethene-oxidizing bacteria).<sup>12–19</sup> The alkene/VC monooxygenase encoded by the *etnABCD* genes initiates VC oxidation and converts VC to chlorooxirane, which is transformed to 2-hydroxyethyl-coenzyme M (CoM) and further catabolized by an epoxyalkane:CoM transferase encoded by *etnE*.<sup>20,21</sup> Under anoxic conditions, organohalide-respiring *Dehalococcoides mccartyi* (*Dhc*) strains and *Dehalogenimonas* (*Dhgm*) *etheniformans* possessing VC reductive dehalogenases (RDases) can utilize VC as the electron acceptor and reductively dechlorinate VC to environmentally benign ethene.<sup>22–27</sup> BA is the butyl ester of acrylic acid and serves as a precursor for synthesizing poly(butyl acrylate), a polymer employed across diverse industries to produce paints, plastics, and acrylic fibers. BA is a colorless liquid with a strong fruity odor and toxic to humans.<sup>28,29</sup> BA is readily biodegraded under oxic conditions;<sup>29–31</sup> however, its fate under anoxic conditions is uncertain.

Natural attenuation of environmental contaminants, driven by physical, chemical, and biological processes, can significantly contribute to remediation and toxicity reduction.<sup>32,33</sup> These natural processes unfold gradually over time in response to environmental perturbations (e.g., contaminant release). Environmental microbiomes harbor microorganisms that can transform, degrade, and detoxify environmental pollutants, including VC and BA. Examining their presence and activities can inform natural attenuation capacity and aid in developing conceptual site models. Molecular biological tools (MBTs), foremost quantitative polymerase chain reaction (qPCR), provide information about the presence and abundance of keystone contaminant-degrading microorganisms and functional genes (i.e., pathways) and are instrumental for site assessment, management, and monitoring.<sup>34–36</sup> For example, quantitatively monitoring the abundances of *Dhc*, *Dhgm*, and VC RDase biomarker genes (i.e., *vcrA*, *bvcA*, *tceA*, and *cera*) can predict ethene formation (i.e., detoxification) at chlorinated solvent sites, and this approach commonly supports the implementation of natural attenuation or enhanced bioremediation.<sup>37–40</sup> The abundances of *etnC* and *etnE* genes have been shown to correlate with VC concentrations in groundwater, highlighting their utility as molecular biomarkers for etheneotroph-mediated aerobic VC biodegradation.<sup>41,42</sup> The quantitative measurement of such biomarker genes can inform about process rates at sites, for which robust conceptual site models have been developed.<sup>43–45</sup> Microcosm treatability studies assess the capacity of the resident microbiome to degrade the contaminants of concern. The value of microcosm studies lies in their ability to directly probe microbial contaminant degradation activity, identify microorganisms and catabolic pathways involved in the processes of interest

(especially when combined with MBTs), and can generate microbial cultures for further study.<sup>46,47</sup>

To obtain information about the presence, abundance, and activity of naturally occurring microorganisms involved in the degradation of VC and BA, sediment, surface water, and well water samples were collected from the East Palestine watershed (Figure S1). MBT application and microcosm treatability studies determined strong biodegradation potential, suggesting that natural attenuation may occur under *in situ* conditions and impact the fate and longevity of VC and BA in the East Palestine watershed.

## MATERIALS AND METHODS

**Chemicals.** VC (purity, >99%) was purchased from SynQuest Laboratories (Alachua, FL, USA). Ethene (>99.9%), butyl acrylate (>99%), *n*-butanol (>99.9%), and acrylic acid (>99.9%) were purchased from Sigma-Aldrich (St. Louis, MO, USA). All other chemicals were at least reagent grade.

**Sample Collection.** Two sampling campaigns collected samples from a total of 17 locations on June 11 (128 days postaccident) and on November 6, 2023 (276 days postaccident) (Table S2). Surface water (SW, total samples *n* = 22) and sediment (SD, total samples *n* = 22) samples were collected from 15 and 12 locations, respectively, including Sulphur Run, Leslie Run, Little Beaver Creek, and other areal waterbodies (see Figure S1 and Table S2 for details). Also sampled were five private drinking water wells (DWs) located along Leslie Run, with some less than 15 m from the waterway (Table S2). Note that three SD/SW sampling locations (i.e., locations 1, 3, and 13) were in proximity to the DW sampling locations and are shown as single locations in Figure S1. The immediate surroundings of the accident site, including the connector stream (Figure S1), were fenced off and not accessible for sample collection (Figure S2A). “Keep Out” signs had been placed at public access points along Sulphur Run downstream of the accident site (Figure S2B), but sampling was possible, with permission, through private properties.

Volumes of approximately 1 L of surface or well water were filtered through Sterivex cartridges (0.22  $\mu$ m, EMD Millipore Corporation, Billerica, MA). The exact volumes filtered were recorded, and the cartridges were immediately transferred to coolers with wet ice and transported to Microbial Insights for DNA extraction and qPCR analysis. Sediment samples were collected by hand using sterilized glass jars and autoclaved stainless-steel spoons. The jars with sediment were topped off with streamwater and closed with gastight lids. The jars were immediately transferred to coolers and kept at 4 °C until further processing.

**Microcosm Treatability Studies.** To examine degradation of VC and BA by native microorganisms, microcosms were established with sediment samples collected in June from 11 locations (i.e., all sediment sampling locations except #17) (Figure S1). VC degradation was examined under both oxic and anoxic conditions, while BA degradation was studied under anoxic conditions without the addition of electron acceptors. Suspension samples (1 mL) from microcosms and transfer cultures were filtered onto a 0.22  $\mu$ m Durapore membrane (Millipore, Cork, Ireland) and stored at –80 °C until DNA extraction for molecular analyses. Details describing the microcosm setup and monitoring are provided in Text S1 and Table S3 (SI).

**Table 1. Detection of Biomarker Genes for Anaerobic (i.e., *Dhc* and *Dhgm* 16S rRNA Genes) and Aerobic (i.e., *etnC* and *etnE*) VC Degradation in Sediment and Surface Water Samples Collected in June (Gray Shading) and November 2023 from Sulphur Run, Leslie Run, and Other Areas Surrounding the East Palestine Derailment Site Using QuantArray High-Throughput qPCR<sup>a</sup>**

Sulphur Run		Sampling campaign	Samples <sup>a,b</sup>								
Target gene			SD-2A	SD-2B <sup>c</sup>	SD-2C	SW-2A	SW-2B	SD-4	SW-4 <sup>c</sup>	SW-7	SD-8
<i>Dhc</i>	Jun	ND	3.8E+3	1.2E+4	4.5E+1	0.3	ND	ND	4.5	ND	5.5
	Nov	ND	4.1E+2	—	0.8	—	1.9E+3	0.3	—	4.9E+2	1.2
<i>Dhgm</i>	Jun	2.1E+6	3.1E+6	6.3E+5	ND	ND	9.6E+6	ND	ND	ND	ND
	Nov	2.2E+4	1.5E+6	—	2.6	—	5.0E+5	2.8	—	1.4E+5	1.5
<i>etnC</i>	Jun	3.9E+4	2.6E+3	ND	ND	ND	8.3E+4	ND	ND	ND	ND
	Nov	ND	1.6E+4	—	ND	—	4.8E+4	ND	—	4.8E+4	ND
<i>etnE</i>	Jun	2.3E+5	ND	ND	ND	ND	1.2E+5	ND	ND	ND	ND
	Nov	ND	ND	—	ND	—	ND	ND	—	6.0E+5	ND
Leslie Run		Sampling event	Samples <sup>a,b</sup>								
Target gene			SD-3	SW-3	SD-6	SW-6	SD-11	SW-11	SD-12	SW-12	SD-15
<i>Dhc</i>	Jun	ND	ND	ND	ND	2.8E+4	5.1	ND	0.4	ND	0.3
	Nov	ND	0.2	—	—	—	—	—	—	—	—
<i>Dhgm</i>	Jun	7.9E+6	ND	ND	ND	1.5E+6	ND	ND	ND	ND	ND
	Nov	ND	0.1	—	—	—	—	—	—	—	—
<i>etnC</i>	Jun	1.1E+5	ND	ND	ND	ND	ND	ND	ND	ND	ND
	Nov	ND	ND	—	—	—	—	—	—	—	—
<i>etnE</i>	Jun	2.6E+5	ND	ND	ND	ND	ND	ND	ND	1.2E+5	ND
	Nov	3.2E+5	ND	—	—	—	—	—	—	—	—
Other locations		Sampling event	Samples <sup>a,b</sup>								
Target gene			SD-1	SW-1	SD-9	SW-9	SD-10	SW-10	SW-13	SW-14	SD-17
<i>Dhc</i>	Jun	1.7E+4	2.3	5.6E+2	—	1.8E+3	ND	ND	ND	1.1E+6	0.3
	Nov	1.4E+3	2.6	8.3E+3	2.3E+1	—	—	—	—	ND	1.1
<i>Dhgm</i>	Jun	ND	ND	6.0E+6	—	3.0E+3	ND	ND	ND	7.8E+6	3.8E+2
	Nov	1.5E+3	1.2E+2	2.7E+5	2.3E+2	—	—	—	—	1.5E+4	9.8
<i>etnC</i>	Jun	ND	ND	ND	—	3.1E+4	ND	ND	ND	1.2E+4	ND
	Nov	ND	ND	ND	ND	—	—	—	—	ND	ND
<i>etnE</i>	Jun	ND	ND	ND	—	ND	ND	ND	ND	ND	ND
	Nov	ND	ND	ND	ND	—	—	—	—	ND	ND

<sup>a</sup>Numbers are reported in units of gene copies g<sup>-1</sup> for sediment (SD) samples or gene copies mL<sup>-1</sup> for surface water (SW) samples. <sup>b</sup>The numbers in the sample designations indicate the sampling location (Figure S1). The capitalized letters A, B, or C indicate multiple sample collections from the same location (collected within a radius of <3 m). ND, not detected. “—”, not sampled. <sup>c</sup>The *bvcA* and *vcrA* genes were not detected in samples collected in June but were detectable, albeit not quantifiable, in November samples.

**DNA Extraction and Quantitative Polymerase Chain Reaction (qPCR).** DNA was isolated from sediments, Sterivex cartridges, and Durapore membrane filters using the DNeasy PowerSoil Kit (Qiagen, Hilden, Germany) following established procedures.<sup>34,48–50</sup> QuantArray high-throughput qPCR assays were used to enumerate (i) *Dhc* and *Dhgm* 16S rRNA genes, (ii) functional genes related to anaerobic chlorinated solvent degradation, including the VC RDase genes *bvcA*, *vcrA*, *tceA*, and *cerA*,<sup>51,52</sup> (iii) the *etnC* and *etnE* genes with roles in aerobic VC catabolism,<sup>20,21,53</sup> and (iv) the adenosine-5'-phosphosulfate reductase gene *apsA* (a biomarker for sulfate reduction).<sup>54</sup> The array plates also included assays to quantify total bacteria 16S rRNA genes.<sup>55,56</sup> qPCR was performed using a QuantStudio 12K Flex real-time PCR system (Applied Biosystems) following validated standard operating procedures. The limit of detection (LOD) and limit of quantification (LOQ) for all qPCR assays are below 100 and 500 cells L<sup>-1</sup>, respectively. The Environmental Microbiology Minimum Information (EMMI) checklist for qPCR assays is provided in the Supporting Information (SI) (Table S4).<sup>57</sup> Additional qPCR information is provided in Text S2 and Table S5 (SI).

**16S rRNA Gene Amplicon Sequencing and Analysis.** Samples collected during the first sampling campaign in June 2023 and from the VC microcosms were analyzed using 16S

rRNA gene amplicon sequencing. 16S rRNA genes were amplified using general primers 341F and 785R targeting the V3–V4 region of bacterial 16S rRNA genes.<sup>58,59</sup> The amplicon library was prepared as described,<sup>58</sup> and sequencing was performed on the Illumina MiSeq platform (San Diego, CA, USA). Sequence data were analyzed using the QIIME 2 2023.7 software package.<sup>60</sup> Raw sequencing reads were jointly paired, demultiplexed, and trimmed to a length of 250 bp using the default plugin DADA2.<sup>61</sup> Representative sequences were used for taxonomic assignments using the default Naïve Bayes Classifier in QIIME 2 against the SILVA v138.1 database.<sup>62,63</sup> Principal coordinate analysis (PCoA) based on Bray–Curtis dissimilarity was calculated in R with packages ggplot2 and phyloseq.<sup>64</sup> Statistical ellipses were calculated using the stat\_ellipse algorithm implemented in the ggplot2 package.<sup>65</sup> PERMANOVA analysis was conducted with the vegan Community Ecology package to evaluate the statistical significance in separation of the microbial communities.<sup>66</sup> The raw amplicon library reads were deposited in the NCBI Sequence Read Archive (SRA) under accessions SAMN42205369–42205402. The taxa identified in sediments, VC-degrading microcosms, and transfer cultures and their relative abundances are listed in Table S6.

**Analytical Procedures.** VC, ethene, BA, and *n*-butanol were analyzed using an Agilent 7890A gas chromatograph equipped with a flame ionization detector (Santa Clara, CA, USA). For VC and ethene measurements, 0.1 mL headspace samples were manually injected,<sup>26</sup> and an Agilent G1888 headspace autosampler (oven temperature, 70 °C; equilibration time, 17 min) was used for BA and *n*-butanol analyses. Acrylate, acetate, and propionate were analyzed by HPLC.<sup>67,68</sup> The oxygen content in the oxic VC microcosms was monitored by manually injecting 1 mL headspace samples into an Agilent 3000A Microgas chromatograph (Palo Alto, CA, USA) equipped with a molecular sieve column coupled with a thermal conductivity detector.

## RESULTS AND DISCUSSION

**Detection of VC Degradation Biomarker Genes in Sediment and Surface Water Samples.** *Dhc* and *Dhgm* 16S rRNA genes were detected in 55% (12 out of 22) and 73% (16 out of 22) of sediment samples in abundances ranging from  $4.1 \times 10^2$  to  $1.1 \times 10^6$  and  $1.5 \times 10^3$  to  $9.6 \times 10^6$  copies  $\text{g}^{-1}$ , respectively (Table 1 and Figure 1). *Dhc* and *Dhgm* 16S rRNA

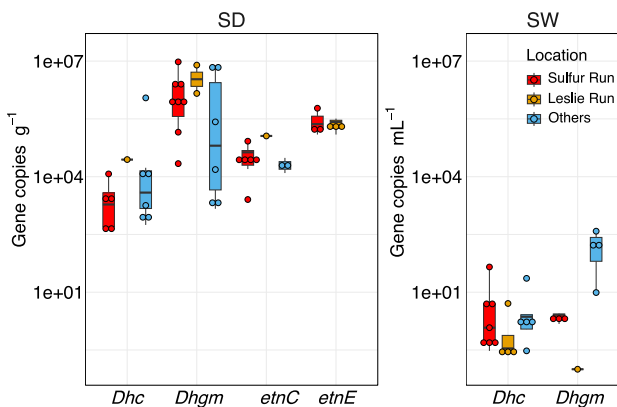


**Figure 1.** Box plot showing the abundances of VC degradation biomarker genes (i.e., *Dhc* and *Dhgm* 16S rRNA genes, *etnC*, and *etnE*) in sediment (SD) and surface water (SW) samples collected from Sulphur Run, Leslie Run, and other locations. The solid circles represent individual measurements, and data from both sampling campaigns are included.

genes were also detected in surface water samples albeit in low abundances ranging from 0.2 to  $4.5 \times 10^1$  and 0.1 to  $3.8 \times 10^2$  copies  $\text{mL}^{-1}$ , respectively (Table 1 and Figure 1). In Sulphur Run (i.e., SD/SW locations 2, 4, 7, and 8, Figure S1), *Dhc* and *Dhgm* detection frequencies (71 and 65% of samples, respectively) exceeded those measured in Leslie Run (42 and 25% of samples, respectively) in both sampling campaigns. Both *Dhc* and *Dhgm* 16S rRNA genes were detected in sediment and surface water samples collected from location 9, about 500 m upstream of the train derailment site during the June and November 2023 sampling campaigns (Table 1). The known VC RDase genes *bvcA*, *tceA*, *vcrA*, and *cerA* were undetectable or below the limit of quantification in the environmental samples (Table 1), despite the detection of *Dhc* and *Dhgm* in abundances reaching  $\sim 10^7$  cells  $\text{g}^{-1}$  of sediment. A possible explanation is that the predominant *Dhc* and *Dhgm* populations harbor yet-to-be identified VC RDase genes. Prior works support the observation that the currently known VC RDase genes do not cover the sequence diversity of this functional clade.<sup>40,39,56</sup>

The *etnC* and *etnE* biomarker genes for aerobic VC degradation were detected in 40 and 27%, respectively, of sediment samples, but were not detected in surface water (Table 1 and Figure 1). The *etnC* and *etnE* genes were detected in Sulphur Run sediment locations 2, 4, and 8 in both sampling campaigns with detection frequencies of approximately 67 and 33%, respectively, and in abundances ranging from  $2.6 \times 10^3$  to  $6.0 \times 10^5$  copies  $\text{g}^{-1}$  (Table 1 and Figure 1). Both aerobic VC degradation biomarker genes were sporadically detected in sediments from Leslie Run and the other locations (Table 1 and Figure 1).

A comparison of biomarker gene abundances in samples collected during the June versus November sampling campaigns (Table 1) revealed a decline of the *Dhgm* population by 2 orders of magnitude, from  $10^6$  to  $10^4$  cells  $\text{g}^{-1}$  in location 2 sediment samples (Sulphur Run, SD-2A). In the same location, the *etnC* and *etnE* gene abundances decreased from  $10^4$ – $10^5$  copies  $\text{g}^{-1}$  measured in June to nondetectable levels in the November samples. Conversely, both aerobic and anaerobic VC degradation biomarker genes increased in sediment collected at location 8 (Sulphur Run, SD-8). Microbial communities are dynamic and respond to environmental stimuli, such as the availability of VC. The EPA reported elevated VC concentrations of up to 8 ppm in Sulphur Run surface water about 5 days following the accident, with subsequently declining concentrations (Figure S3).<sup>6</sup> Surface water monitoring started with several days delay, and peak contaminant concentrations were likely missed. Data for VC in streambed sediment are not available, but it is likely that elevated contaminant concentrations occurred for some time following the accident. The frequent detection and elevated abundances of VC degradation biomarker genes in sediment samples collected from Sulphur Run suggest a microbial response to the perturbation (i.e., the influx of VC).

Variability in the detection and the abundances of biomarker genes was observed in sediment samples collected from the same sampling location (e.g., Sulphur Run location 2; Table 1). The high variability within a location highlights the heterogeneous nature of the streambeds, and *Dhc* abundances differed by orders of magnitude in samples collected short distances apart. Intermittent water flow was observed in the connector stream and Sulphur Run (Figure S1), with water levels strongly impacted by rain events and water releases from makeshift dams that Norfolk Southern contractors installed to control water flow. During the June sampling campaign, Sulphur Run had stagnant pools of water without continuous flow, which dramatically changed following an overnight rain event (Figure S4). Dynamic changes of the environment and a heterogeneous distribution of microorganisms highlight the importance of early and regular time-series sampling at multiple locations for a robust interpretation of MBT data. Another consideration is the potential presence of legacy contaminants. To our knowledge, there is no available information on chlorinated solvent contamination affecting Sulphur Run and connected streams prior to the 2023 train derailment (Table S7), although undocumented releases cannot be ruled out. Prior exposure to, e.g., chlorinated solvents could have selected for VC degraders and primed the sediment microbiomes for VC attenuation. For example, the detection of high abundances of both *Dhc* and *Dhgm* in Little Beaver Creek samples collected near the junction with the Ohio River (location 17), approximately 20 km downstream of the derailment site, might reflect other contaminant sources.

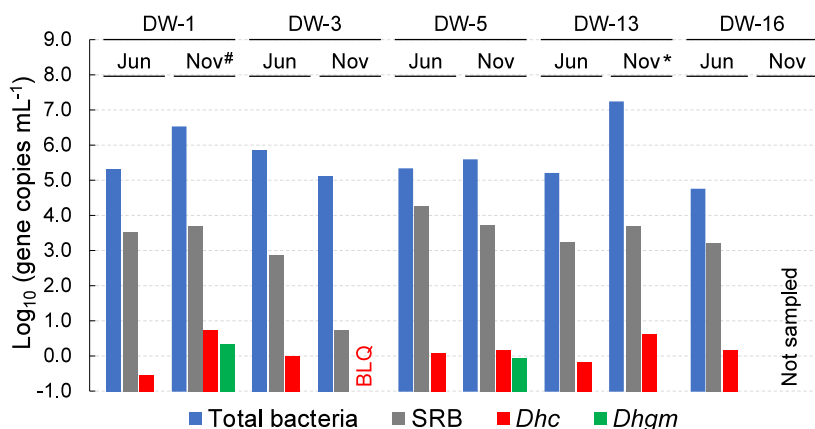


**Figure 2.** Abundances of total bacteria, SRB, *Dhc*, and *Dhgm* determined with qPCR, in the five drinking water wells (DWs) sampled in June and November 2023. BLQ, *Dhc* was detected but below the limit of quantification. #, *bvcA* and *vcrA* genes were detected in abundances of 1.2 and 2.1 copies  $\text{mL}^{-1}$ , respectively. \*, *bvcA* and *vcrA* genes were detected but BLQ.

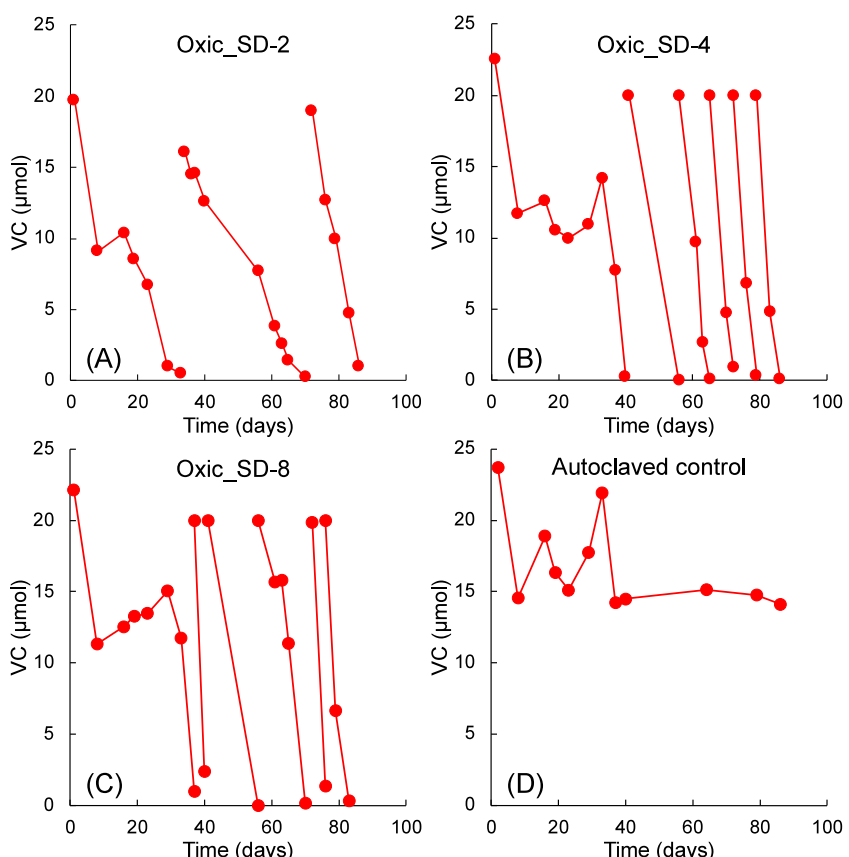


**Figure 3.** VC degradation in oxic streambed sediment microcosms. Panels A–C show microcosms established with Sulphur Run sediments collected from locations 2, 4, and 8. Representative data for single microcosms are depicted, and the performances of replicates and other microcosms are shown in Figure S5. Some VC loss was observed in autoclaved controls, but at least 60% of the initial VC dose remained at the end of the incubation period (D).

**Detection of VC Degradation Biomarker Genes in Drinking Water Wells.** A surprising finding was that *Dhc* 16S rRNA genes were quantifiable, albeit in low abundances ranging from 0.3 to 5.6 copies  $\text{mL}^{-1}$ , in all residential DWs sampled (June,  $n = 5$ ; November,  $n = 4$ ) (Figure 2). *Dhgm* 16S rRNA genes were not detected in any samples collected in June but quantifiable in DW-1 and DW-5 samples collected in November 2023 (Figure 2). No VC RDase genes were detected in the well water samples collected in June; however,

both *bvcA* and *vcrA* were detectable and quantifiable in DW-1 in samples collected in November (Figure 2). The *bvcA* and *vcrA* genes were also detected in the DW-13 sample collected in November, albeit below the quantification limit. The aerobic VC degradation biomarker genes *etnC* and *etnE* were not detected in well water. VC was never reported to occur in drinking water wells, suggesting that *Dhc* and *Dhgm*, both strictly organohalide-respiring bacteria (OHRB), did not grow in the wells. The presence of *Dhc* and *Dhgm* in well water

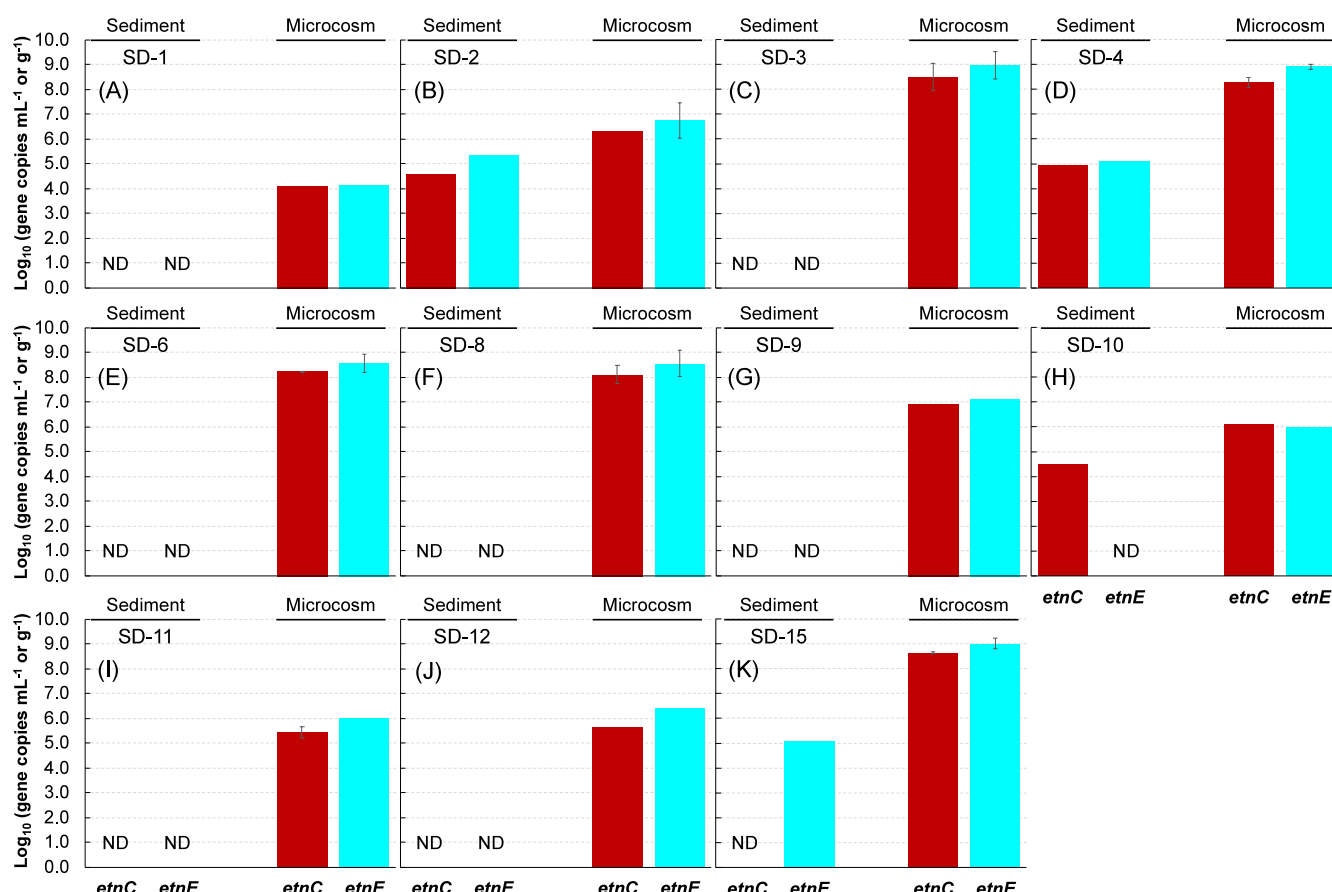


**Figure 4.** qPCR enumeration of the aerobic VC degradation biomarker genes *etnC* and *etnE* in 11 sediment samples and the corresponding oxic, VC-degrading microcosms. Data from microcosms SD-2 (panel B), SD-3 (C), SD-4 (D), SD-6 (E), SD-8 (F), SD-11 (I), and SD-15 (K) represent the averages of duplicate microcosms, and the error bars show the standard deviation. Data for the original sediments and microcosms SD-1 (A), SD-9 (G), SD-10 (H), and SD-12 (J) are from nonreplicated samples. ND, not detected.

could be a symptom of an OHRB bloom in the streambed sediment and the subsurface following the release of VC. Such *Dhc* and *Dhgm* blooms would increase the number of planktonic cells being transported with the groundwater flow, apparently reaching drinking water wells.<sup>69</sup> Residents reported a rotten egg smell and taste of their well water that was not observed prior to the train derailment, suggesting a connection between the release of contaminants and the appearance of hydrogen sulfide in the DWs. An on-site rapid bismuth subsalicylate test confirmed the presence of sulfide in well water via the observable formation of dark-brown bismuth sulfide.<sup>70</sup> Organic compounds, including BA and glycols, released in the accident, as well as ethene (i.e., the product of VC reductive dechlorination) can stimulate sulfate reduction associated with the formation of hydrogen sulfide.<sup>71</sup> Consistently, qPCR detected sulfate-reducing bacteria (SRB) in all DW samples reaching abundances of  $\sim 10^4$  cells mL<sup>-1</sup> (Figure 2). These observations were made in shallow (DW-3, <7.6 m depth) and deep (DW-1, DW-5, DW-13, and DW-16, 23–46 m depth) DWs, suggesting that both shallow and deep wells were impacted by disturbances caused by the accident. The probable connection between surface water and groundwater feeding shallow and deep wells highlights the importance of hydrogeological information, which could have helped to predict the transport of contaminants and transformation products in the East Palestine watershed.

**Aerobic VC Degradation.** Live oxic microcosms established with sediments from 11 sampling locations (Table S3) consumed VC after lag phases of 20–40 days. VC was completely degraded after incubation periods of 40–80 days (Figure 3 and Figure S5). Additional VC feedings were consumed without an apparent lag phase at accelerating rates consistent with acclimated microbiomes. Microcosms established with sediments from Sulphur Run locations 4 and 8 exhibited the highest VC degradation rates of 50–200  $\mu\text{M}$  day<sup>-1</sup> (Figure 3). An initial loss of VC was observed in all oxic microcosms, including the heat-killed controls; however, at least 60% of the initial VC dose remained in the control microcosms following a 90-day incubation period (Figure 3).

16S rRNA gene amplicon sequencing revealed the presence of genera known to harbor VC oxidizers. *Mycobacterium* sequences were detected in all oxic VC-degrading microcosms except one replicate from location 2 (Oxic\_SD-2\_R2, Table S8). In nine of the 13 oxic VC-degrading microcosms, *Mycobacterium* sequences dominated the sequence pool with relative abundances reaching 35% (Table S8). Sequences representing other genera linked to VC oxidation (i.e., *Nocardioides*, *Pseudomonas*, *Ralstonia*, and *Rhodococcus*) were detected in some microcosms at low relative abundances. In the original sediments used for the microcosm setup, *Mycobacterium* amplicons were detected in low abundances in sediment samples from locations 3 and 15 (Table S9). *Nocardioides*, *Rhodococcus*, and *Pseudomonas* sequences had low

relative abundances, and these taxa were not enriched in any of the VC-degrading oxic microcosms (Table S9). While the microcosm data attribute *Mycobacterium* a key role in aerobic VC degradation, it is possible that the enrichment process (e.g., medium composition) introduced a bias, and a broader diversity of etheneotrophs contributes to VC consumption under *in situ* conditions.

qPCR assays detected the aerobic VC degradation biomarker genes *etnC* and *etnE* in abundances ranging from  $1.2 \times 10^4$  to  $4.4 \times 10^8$  and from  $1.4 \times 10^4$  to  $1.0 \times 10^9$  copies  $\text{mL}^{-1}$  of culture suspension, respectively, in all oxic, VC-degrading microcosms (Figure 4). In the original sediments used for the microcosm setup, the *etnC* and *etnE* biomarker genes were only detected in Sulphur Run sediment samples SD-2 and SD-4 in abundances ranging from  $3.9 \times 10^4$  to  $2.3 \times 10^5$  copies  $\text{g}^{-1}$  (Figure 4), demonstrating the enrichment of *etnC*- and *etnE*-harboring VC-degrading microorganisms after repeated VC feedings.

Aerobic VC degradation was prevalent, consistent with prior research, where aerobic VC degradation was detected in 23 of 37 microcosms established with samples from different chlorinated solvent impacted sites.<sup>72,73</sup> The lag phases for the onset of aerobic VC oxidation in the East Palestine microcosms ranged between 20 and 40 days, significantly shorter than the average lag phase of  $\sim 60$  days reported in the literature.<sup>72,74,75</sup> A plausible explanation for the shorter lag phases could be the exposure to VC and priming of the streambed microbiomes prior to the microcosm setup. *Mycobacterium* populations dominated most oxic VC microcosms, which is consistent with prior findings, where *Mycobacterium* strains were frequently enriched and isolated from oxic, VC-degrading microcosms.<sup>72</sup> These findings emphasize the potential significance of *Mycobacterium* strains for natural attenuation of VC under oxic conditions. In addition to metabolic VC degradation by etheneotrophs, VC is also susceptible to cometabolism by widely distributed bacteria such as methanotrophs.<sup>15,21,76,77</sup>

**Anaerobic VC Biodegradation.** Reductive dechlorination of VC to ethene was observed in anoxic microcosms established with Sulphur Run sediments collected at locations 2, 4, and 8 (Figure 5 and Figure S6). VC-to-ethene reductive dechlorination commenced after 10–20 days in microcosms SD-4 and SD-8 and after  $\sim 40$  days in microcosm SD-2. VC was completely consumed after incubation periods of 20–60 days and converted to near stoichiometric amounts of ethene. Additional VC feedings were dechlorinated to ethene without an apparent lag phase at higher rates of  $15\text{--}25 \mu\text{M day}^{-1}$  in microcosms SD-2 and SD-8 and  $\sim 100 \mu\text{M day}^{-1}$  in microcosm SD-4. VC degradation and ethene formation were not observed in anoxic microcosms established with sediments collected along Leslie Run and the pond located  $\sim 500$  m east of the derailment site (i.e., location 9, Figure S1) even after an extended incubation period of 8 months, except for one replicate microcosm (i.e., Anoxic\_SD-15). The comparatively short lag phases observed in microcosms established with Sulphur Run sediments suggest prior *in situ* enrichment of VC-dechlorinating OHRB, presumably due to VC exposure, before samples were collected in the first sampling campaign. Reductive dechlorination of VC was not observed in microcosms established with sediments collected upstream (i.e., location 9) and further downstream (i.e., Leslie Run) of the derailment site, possibly because prior VC exposure and enrichment of VC dechlorinators did not occur. Interestingly,

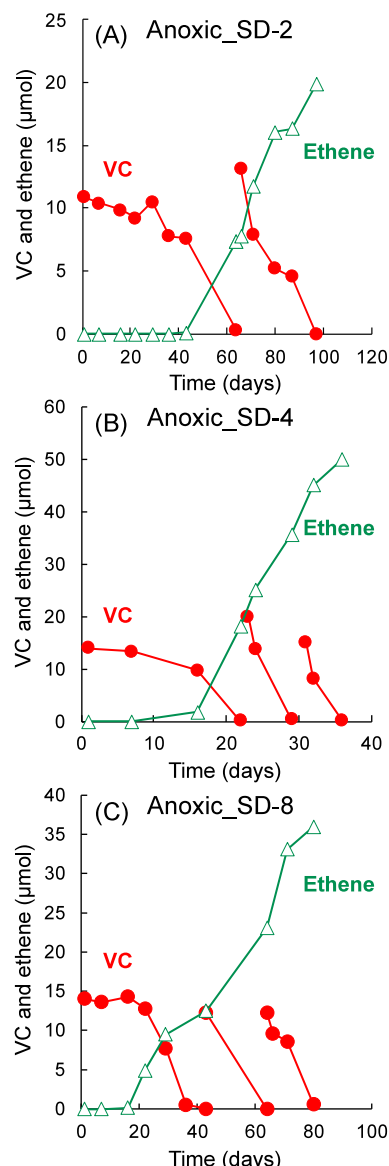


**Figure 5.** Reductive dechlorination of VC to ethene in anoxic microcosms established with Sulphur Run sediments collected from locations 2 (A), 4 (B), and 8 (C). Representative data for single microcosms are depicted, and the performances of replicate microcosms are shown in Figure S6.

the molecular analysis demonstrated the presence of *Dhc* and *Dhgm* in location 9 and some Leslie Run sediment samples (Table 1), but these OHRB apparently lack the VC dechlorination phenotype. All anoxic microcosms produced methane, indicating that reducing conditions conducive to OHRB activity had established. The lack of VC reductive dechlorination activity in some of the microcosms may be due to the absence or low abundance of VC-dechlorinating OHRB and the prevalence of methanogenic activity.

16S rRNA gene amplicon sequencing performed with DNA extracted from the original sediments, the VC-dechlorinating microcosms, and the first transfer cultures revealed increasing abundances of *Dhc* in response to enrichment with VC (Table S10). The analysis detected sequences representing the order *Dehalococcoidales* in the original sediments collected in June from locations 2 and 9, both close to the derailment site (Figure S1), with relative abundances of 0.1 and 0.6% (Table

S6), respectively, but none of these sequences could be assigned to the genera *Dhc* or *Dhgm*. In anoxic VC-dechlorinating microcosms SD-2, SD-4, and SD-8 and the first-generation transfer cultures, the relative abundances of *Dhc* sequences increased to 0.2–0.5 and 3.6–5.7%, respectively (Table S10). *Dhgm* sequences were detected in anoxic, VC-dechlorinating SD-2 microcosms with relative abundances of 0.2%; however, *Dhgm* were not enriched in VC-dechlorinating transfer cultures (Table S10).

Even though qPCR did not detect the *Dhc* 16S rRNA gene and VC RDase genes in the original sediments (Figure 6),

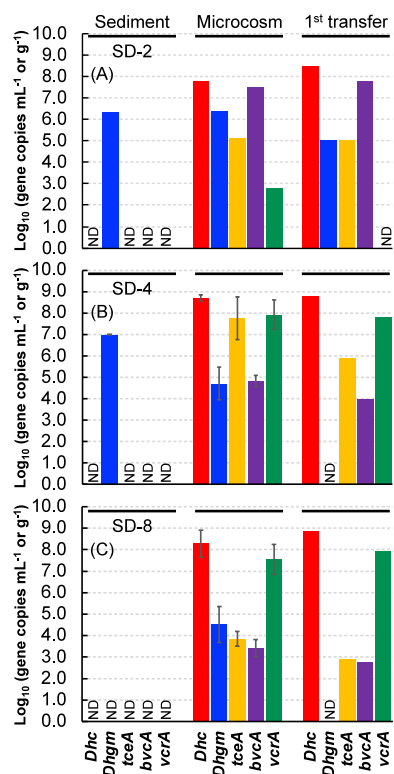


**Figure 6.** Detection of anaerobic VC degradation biomarker genes, i.e., *Dhc* and *Dhgm* 16S rRNA genes, and VC RDase genes *tceA*, *bvcA*, and *vcrA* in sediment samples SD-2A (A), SD-4 (B), and SD-8 (C), the corresponding anoxic, VC-degrading microcosms, and the first-generation transfer cultures using qPCR. Data shown for microcosms SD-4 (B) and SD-8 (C) are averages from duplicate microcosms, and the error bars represent the standard deviation. Data for the three original sediments used for the microcosm setup, microcosm 2-SD (A), and the first-generation transfer cultures of SD-2 (A), SD-4 (B), and SD-8 (C) represent nonreplicated samples. ND, not detectable. Gene abundances are shown in gene copies  $\text{g}^{-1}$  (sediments) or copies  $\text{mL}^{-1}$  (microcosms and first-generation transfer cultures).

microcosms SD-2, SD-4, and SD-8 dechlorinated VC to ethene. Following enrichment with VC as the electron acceptor, *Dhc* 16S rRNA gene abundances reached an average of  $3.9 \times 10^8$  copies  $\text{mL}^{-1}$ , and *tceA*, *bvcA*, and *vcrA* reached average abundances of  $1.6 \times 10^7$ ,  $4.3 \times 10^6$ , and  $5.7 \times 10^7$  copies  $\text{mL}^{-1}$ , respectively, in the active anoxic microcosms and the first-generation transfer cultures (Figure 6). qPCR detected the *Dhgm* 16S rRNA gene in the original sediment samples from locations 2 and 4 and in the dechlorinating microcosms SD-2, SD-4, and SD-8; however, *Dhgm* biomarkers, including the 16S rRNA gene and the VC RDase gene *cerA*,<sup>25,26</sup> were not detected in transfer cultures, suggesting that *Dhgm* did not

contribute to the VC-to-ethene reductive dechlorination activity observed in the microcosms, a conclusion consistent with the 16S rRNA gene amplicon sequencing results (Table S10). The findings highlight the advantages of target-specific qPCR over 16S rRNA gene amplicon sequencing, with qPCR providing higher sensitivity (i.e., lower LOD than amplicon sequencing) and absolute quantification (versus merely relative abundance information on the amplicon sequencing approach).

Enrichment with VC under oxic or anoxic conditions led to notable changes in microbial community structures and the increase in taxa implicated in VC degradation (Figure S7). The enrichment of both aerobic and anaerobic VC-degrading bacteria demonstrates the adaptive capacity and resilience of microbiomes to perturbations. *Dhc* populations harboring VC RDase genes are keystone bacteria for VC detoxification<sup>24</sup> and were rapidly enriched in all active anoxic microcosms (Figure 6). In addition to *Dhc*, *Dehalogenimonas etheniformans* performs VC-to-ethene reductive dechlorination.<sup>26,27</sup> *Dhgm* was initially present in the sediments at an abundance of  $\sim 10^6$  copies  $\text{g}^{-1}$ , and *Dhgm* outnumbered *Dhc* in 16 out of 22 sediment samples (Table 1). Upon laboratory enrichment, *Dhgm* declined whereas *Dhc* increased in abundance (Figure 6). It is not uncommon that *Dhgm* outnumbered *Dhc* at contaminated sites, but procedures aimed at enriching OHRB generally favor *Dhc* over *Dhgm*.<sup>25,40</sup> Current protocols to enrich strict OHRB apparently select *Dhc* over *Dhgm*, emphasizing the need for developing cultivation procedures that favor non-*Dhc* OHRB.

#### Microbial Degradation of Butyl Acrylate (BA).

Following the accident, BA was detected within the watershed with a maximum dissolved concentration of 180 ppm reported for Sulphur Run (Figure S8).<sup>6</sup> BA can be readily degraded under oxic conditions by ubiquitous bacteria;<sup>29–31</sup> however, its fate under anoxic conditions is less clear. BA degradation occurred in all anoxic microcosms without the addition of an external electron acceptor. The initial amount of  $\sim 35 \mu\text{mol}$  BA  $\text{bottle}^{-1}$  (aqueous phase concentration,  $\sim 1.14 \text{ mM}$ ; Text S1) was consumed within 1–3 weeks without an apparent lag phase, with a transient formation of *n*-butanol (maximum measured concentration of  $28.8 \pm 1.7 \mu\text{mol} \text{ bottle}^{-1}$ ) (Figure 7 and Figure S9). Lower BA degradation rates were observed in microcosms established with sediments from locations 1 and 6, and *n*-butanol accumulated over a 3-week incubation period (Figure S9). BA-degrading transfer cultures could be readily obtained from BA-degrading microcosms, and HPLC analysis performed on second-generation transfer cultures identified acrylate as an additional intermediate of BA degradation (Figure 7). The second-generation transfer cultures completely degraded  $\sim 35 \mu\text{mol}$  BA within a 3-day incubation period, and the transformation intermediates acrylate and *n*-butanol were subsequently consumed, with methane and acetate measured as products (Figure 7).

The ester bond of BA is susceptible to enzymatic hydrolysis,<sup>78,79</sup> leading to the formation *n*-butanol and acrylate, which are compounds of lower environmental concern and degradable under oxic and anoxic conditions.<sup>31</sup> In anoxic environments deplete of electron acceptors, the degradation of *n*-butanol might require syntrophic partnerships, resulting in slow kinetics and turnover.<sup>80</sup> Elevated concentrations of *n*-butanol and acrylate slowed BA degradation in microcosms SD-1 and SD-6 (Figure S9), possibly pointing at product inhibition of the initial hydrolysis step. The conversion of

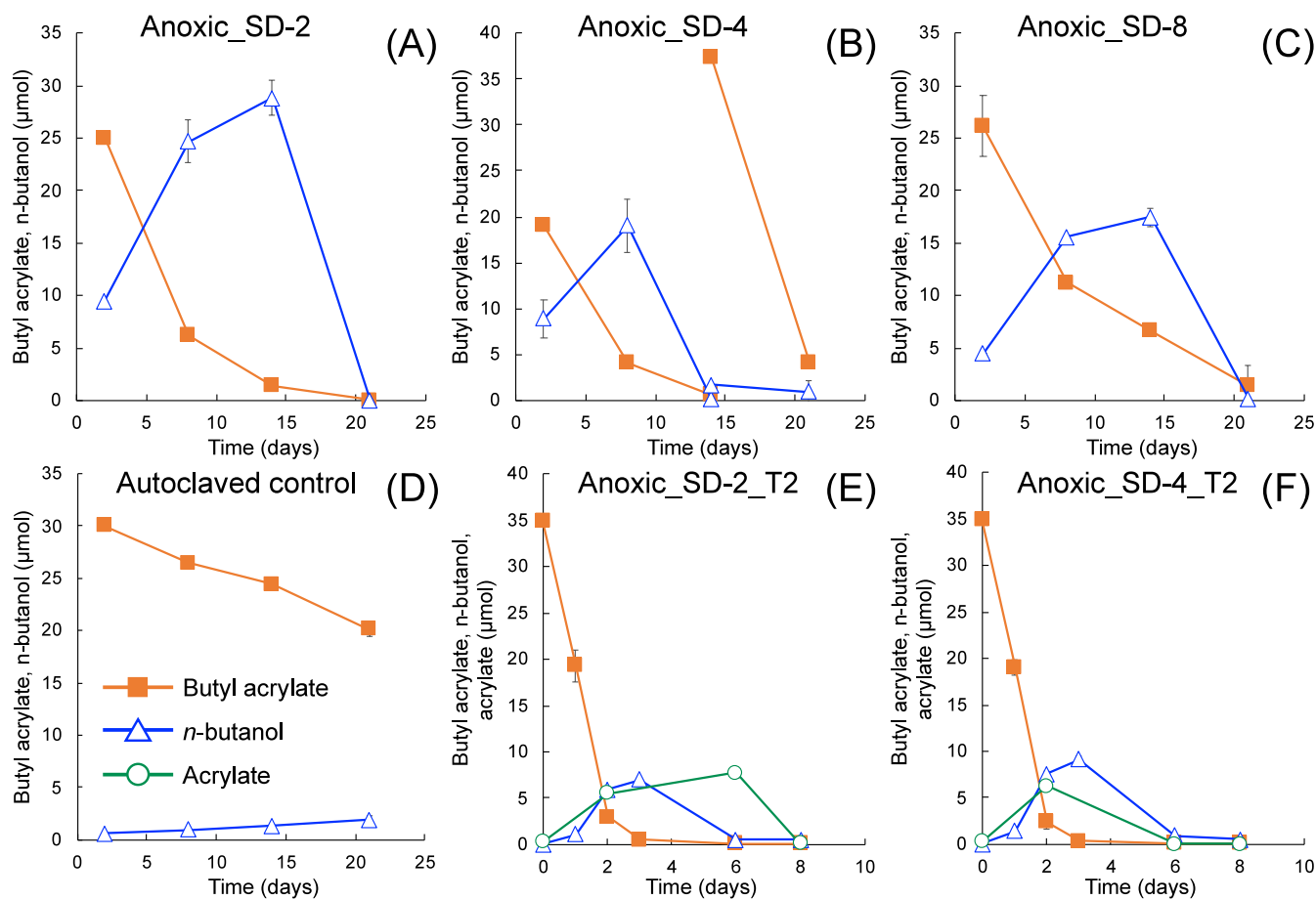


**Figure 7.** Degradation of butyl acrylate (BA) and the transient formation of *n*-butanol in anoxic microcosms established with sediments from Sulphur Run sampling locations 2, 4, and 8 (A–C). Some loss of BA and the formation of small amounts of *n*-butanol were observed in heat-killed control microcosms, presumably due to sorption and abiotic processes (D). Panels E and F show the transient formation of acrylate and *n*-butanol during BA degradation in second-generation transfer cultures derived from microcosms SD-2 and SD-4. The data represent the averages of duplicate incubations, and the error bars represent the standard deviation. Error bars are not shown when they are smaller than the symbol.

acrylate to lactate, followed by fermentation to acetate and propionate under anoxic conditions, represents a biodegradation pathway for acrylate that has been demonstrated in environmental, microcosm, and pure culture studies.<sup>81–84</sup> The treatability study demonstrated BA hydrolysis to *n*-butanol and acrylate in all microcosms, and subsequent acrylate fermentation and syntrophic fatty acid oxidation can lead to the complete detoxification of BA in anoxic environments (Figure S10). Considering the likelihood of comingled BA and VC in the East Palestine watershed, BA fermentation can potentially supply electron donors for VC reductive dechlorination through metabolite cross-feeding (e.g., H<sub>2</sub> and formate).<sup>85,86</sup>

**Recommendations.** The East Palestine derailment is not an isolated incident, and train accidents associated with major VC spills have historically occurred once per decade, as documented by accidents in Livingston, LA in 1982 (>450 t VC released), in Schönbeck, Germany in 1996 (~700 t, of which 261 t were burned), in Paulsboro, NJ in 2012 (~90 t), and East Palestine, OH in 2023 (~450 t). VC is the precursor for the polymer PVC, and the VC global market size exceeded 52 million t in 2022 with a projected average annual growth rate of 2%.<sup>87</sup> Transporting toxic precursor petrochemicals such as VC bears an inherent risk that can be eliminated, or at least minimized, if manufacturing and processing industries would be colocated. While not achievable in the short term, strategic

planning could reduce risks associated with the transportation of toxic materials.

The intensity of the accident required quick decision-making and resulted in the improvised burn of predominantly VC, other petrochemicals, and PVC (Table S1). This VC burn was also executed in the aftermath of the Livingston train derailment. Incomplete combustion generates undesirable byproducts including acrolein, polycyclic aromatic hydrocarbons (PAHs), PCDDs, PCDFs, and other toxins, each carrying its own set of environmental and human health risks.<sup>2,7,88–90</sup> Atmospheric dispersion and transport of particulates affected local air quality in downwind regions, effectively impacting a much larger area than the original spill.<sup>3</sup> Even more troubling, PCDDs and PCDFs are recalcitrant toxins, and several congeners are strong carcinogens with bioaccumulation and biomagnification potential. Initial measurements suggest that high concentrations of PCDDs may occur in soils collected in East Palestine, underscoring the potential impact of the chosen first-response strategy.<sup>91</sup> Information is emerging indicating that the burn decision was based on false assumptions, and the perceived danger of uncontrolled VC polymerization and an imminent explosion never existed.<sup>92</sup> Pumping the VC from the damaged tank cars into suitable containers (e.g., new tank cars) could have effectively circumvented the formation of highly dangerous

toxins associated with the burn. The burn provided a solution to quickly return to normal railroad operations with clear economic benefits; however, the trade-off adopted is the uncertainty associated with lingering PCDDs and PCDFs and potentially long-lasting impacts on human and environmental health.<sup>93</sup> The burn of VC, BA, and other materials, including PVC, likely resulted in the formation of toxic combustion byproducts, and continued short- and long-term monitoring regimes for toxins such as PCDDs and PCDFs are essential for protecting human and environmental health.

For any incident involving the environmental release of water-soluble pollutants, such as VC and BA, particularly when nearby surface and drinking water receptors are impacted, available hydrogeological information can predict contaminant transport and alert residents of potential dangers associated with drinking water usage. Even though EPA monitoring has not detected contaminants in drinking water wells, the detection of OHRB and SRB biomarker genes and hydrogen sulfide strongly suggests that disruptions resulting from the accident have impacted and possibly continue to impact wells. The availability of hydrogeological data could have improved decision-making and instilled residents' confidence in drinking water safety.

Microcosm treatability studies and qPCR provide complementary information and highlight the potential for natural attenuation of VC and BA in the East Palestine watershed. Although our study did not measure or demonstrate *in situ* VC and BA degradation, the laboratory studies suggest strong natural attenuation potential for these compounds, which should be considered in site management decision-making. Ideally, data from both laboratory studies and field measurements (e.g., compound-specific isotope analysis (CSIA) and detection of process-specific transformation products) would be available to document natural attenuation. We intended to perform CSIA to measure the potential enrichment of <sup>13</sup>C-VC during biodegradation.<sup>94</sup> However, our initial sampling event occurred in June 2023, more than 4 months after the accident, at which time the VC concentrations had declined to levels not allowing meaningful CSIA and data interpretation. Of note, during this period, several remedial practices, such as aeration and removal of surface soil and sediment, had been conducted at the site. Although the NSF Rapid Response Research (RAPID) funding mechanism is fast-tracked, the opportunity for early field measurements was missed. Earlier sampling could have provided a deeper insight into the dynamic responses of the resident microbiomes to the accidental release of contaminants that may have aided the implementation of refined decision-making strategies. Norfolk Southern contractors collected samples following the accident, and the inclusion of such samples could have provided a clearer picture of the microbial responses following the spill. Unfortunately, the authors were unable to obtain access to samples collected prior to June 2023.

Considering that VC spills are reoccurring events, it is surprising that emergency assessment and guidance documents for decision-making following environmental accidents of this type are not readily available. Manufacturers of VC, the U.S. Department of Transportation (which regulates the transportation of toxic chemicals), toxicologists, and environmental scientists and engineers have the opportunity (mandate) to develop guidance documents that provide clear information to decision makers and first responders for implementing solutions that best protect human and environmental health.

The Interstate Technology and Regulatory Council (ITRC) could provide experts a forum to develop such guidance documents.

Lastly, unambiguous and diverse forms of communication are essential when providing information to impacted community members. The East Palestine accident demonstrated that a lack of understandable, nontechnical communication leads to misconception, misinterpretation, and confusion and quickly erodes trust in science and government. The issues that have arisen when attempting to communicate essential information to the East Palestine community should trigger an investigation with the goal of enhancing existing protocols and developing improved response capabilities by a competent expert authority.

## ASSOCIATED CONTENT

### Supporting Information

The Supporting Information is available free of charge at <https://pubs.acs.org/doi/10.1021/acs.est.4c04198>.

Text S1 and Text S2, 10 tables, and 10 figures: microcosm setup and monitoring methodologies (Text S1); qPCR methodologies (Text S2); partial train manifest (Table S1); sampling location and sample information (Table S2); list of VC and BA microcosms (Table S3); EMMI checklist for qPCR (Table S4); qPCR metadata (Table S5); list of prior environmental spills potentially affecting Sulphur Run and Leslie Run (Table S7); relative abundances of potential aerobic VC degraders in oxic microcosms (Table S8); relative abundances of potential aerobic VC degraders in the original sediment samples (Table S9); relative abundances of *Dhc* and *Dhgm* in anoxic, VC-dechlorinating microcosms (Table S10); sampling map (Figure S1); restricted creek access near the accident site (Figure S2); VC concentration data in surface water monitored by the Ohio EPA (Figure S3); variable water levels in Sulphur Run (Figure S4); VC degradation in oxic microcosms (Figure S5); reductive dechlorination of VC to ethene in anoxic microcosms (Figure S6); PCoA analysis of the microbial community composition of anoxic and oxic VC-degrading microcosms and of the original sediment samples (Figure S7); BA concentration data in surface water monitored by the Ohio EPA (Figure S8); BA degradation and *n*-butanol formation in anoxic microcosms amended with BA (Figure S9); illustration of BA degradation under anoxic conditions (Figure S10) ([PDF](#))

Relative abundances of taxa identified in sediments, microcosms, and transfer cultures (Table S6) ([XLSX](#))

## AUTHOR INFORMATION

### Corresponding Author

Frank E. Loeffler – Department of Civil and Environmental Engineering, The University of Tennessee Knoxville, Knoxville, Tennessee 37996, United States; Department of Microbiology and Department of Biosystems Engineering and Soil Science, The University of Tennessee Knoxville, Knoxville, Tennessee 37996, United States; [orcid.org/0000-0002-9797-4279](https://orcid.org/0000-0002-9797-4279); Phone: (865) 974-4933; Email: [frank.loeffler@utk.edu](mailto:frank.loeffler@utk.edu)

## Authors

**Gao Chen** — *Department of Civil and Environmental Engineering, The University of Tennessee Knoxville, Knoxville, Tennessee 37996, United States; [orcid.org/0000-0002-8767-3130](https://orcid.org/0000-0002-8767-3130)*

**Sam Rosolina** — *Microbial Insights, Incorporated, Knoxville, Tennessee 37932, United States*

**Elizabeth Padilla-Crespo** — *Science and Technology Department, Inter American University of Puerto Rico, Aguadilla 00605, Puerto Rico; [orcid.org/0000-0002-1038-3987](https://orcid.org/0000-0002-1038-3987)*

**Guang He** — *Department of Civil and Environmental Engineering, The University of Tennessee Knoxville, Knoxville, Tennessee 37996, United States*

**Qiao Chen** — *Department of Civil and Environmental Engineering, The University of Tennessee Knoxville, Knoxville, Tennessee 37996, United States*

**Ana Arosemena** — *Science and Technology Department, Inter American University of Puerto Rico, Aguadilla 00605, Puerto Rico*

**Bryan E. Rosado-Maldonado** — *Science and Technology Department, Inter American University of Puerto Rico—Metropolitan Campus, San Juan 00926, Puerto Rico*

**Cynthia M. Swift** — *Department of Civil and Environmental Engineering, The University of Tennessee Knoxville, Knoxville, Tennessee 37996, United States*

**Paula Belmont Coelho** — *Division of Environmental and Ecological Engineering, College of Engineering, Purdue University, West Lafayette, Indiana 47907, United States*

**Andrew J. Whelton** — *Division of Environmental and Ecological Engineering, College of Engineering, Purdue University, West Lafayette, Indiana 47907, United States*

**Dora Taggart** — *Microbial Insights, Incorporated, Knoxville, Tennessee 37932, United States*

Complete contact information is available at:

<https://pubs.acs.org/10.1021/acs.est.4c04198>

## Notes

The authors declare no competing financial interest.

## ACKNOWLEDGMENTS

This work was supported by the U.S. National Science Foundation (NSF) through Rapid Response Research (RAPID) (Awards 2325719 and 2327139). REU students A.A. and B.E.R.-M. were supported by NSF award 1831599. E.P.-C. acknowledges support from the U.S. Department of Energy, Office of Science, Office of Workforce Development for Teachers and Scientists (WDTs) under the Visiting Faculty Program (VFP) program at Oak Ridge National Laboratory, administered by the Oak Ridge Institute for Science and Education. Our team is indebted to the brave residents of East Palestine for logistical support, providing access to sampling locations, many informative discussions, their genuine interest in scientific research, and unwavering endurance following the accident.

## REFERENCES

- (1) National League of Cities (NLC). *Interactive Rail Safety Map: See Derailments in Communities Across the U.S.* <https://www.nlc.org/resource/interactive-rail-safety-map-see-derailments-in-communities-across-the-u-s/>.
- (2) Wang, B.; Heng, L.; Sui, Q.; et al. Insight of chemical environmental risk and its management from the vinyl chloride accident. *Front Environ. Sci. Eng.* **2023**, *17*, 52.
- (3) Gay, D. A.; Blaydes, K.; Schauer, J. J.; et al. Widespread impacts to precipitation of the East Palestine Ohio train accident. *Environ. Res. Lett.* **2024**, *19*, No. 074022.
- (4) Runwal, P. Visiting East Palestine 1 year later. *C&EN (Chemical Eng. News)* **2024**, *102*, 24–34.
- (5) NewsNation. *Plane Passenger Photo Shows Size of Smoke Plume After Ohio Train Derailment.* <https://www.newsweek.com/plane-passenger-photo-smoke-plume-ohio-train-derailment-1781722>.
- (6) Ohio EPA. *East Palestine Train Derailment Information.* <https://epa.ohio.gov/divisions-and-offices/surface-water/reports-data/ep-surface-water-results>.
- (7) Lenharo, M. Ohio train derailment: scientists scan for lingering toxics. *Nature* **2023**.
- (8) Cogliano, V. J.; Hiatt, G. F. S.; Den, A. Quantitative cancer assessment for vinyl chloride: indications of early-life sensitivity. *Toxicology* **1996**, *111*, 21–28.
- (9) Kielhorn, J.; Melber, C.; Wahnschaffe, U.; et al. Vinyl chloride: still a cause for concern. *Environ. Health Perspect* **2000**, *108*, 579–588.
- (10) US EPA. *National primary drinking water regulations.* <https://www.epa.gov/ground-water-and-drinking-water/national-primary-drinking-water-regulations#one>.
- (11) Danso, D.; Chow, J.; Streit, W. R. Plastics: environmental and biotechnological perspectives on microbial degradation. *Appl. Environ. Microbiol.* **2019**, *85*, e01095–19.
- (12) Hartmans, S.; De Bont, J. A. Aerobic vinyl chloride metabolism in *Mycobacterium Aurum* L1. *Appl. Environ. Microbiol.* **1992**, *58*, 1220–1226.
- (13) Malachowsky, K. J.; Phelps, T. J.; Teboli, A. B.; et al. Aerobic mineralization of trichloroethylene, vinyl chloride, and aromatic compounds by *Rhodococcus* species. *Appl. Environ. Microbiol.* **1994**, *60*, 542–548.
- (14) Verce, M. F.; Ulrich, R. L.; Freedman, D. L. Characterization of an isolate that uses vinyl chloride as a growth substrate under aerobic conditions. *Appl. Environ. Microbiol.* **2000**, *66*, 3535–3542.
- (15) Verce, M. F.; Ulrich, R. L.; Freedman, D. L. Transition from cometabolic to growth-linked biodegradation of vinyl chloride by a *Pseudomonas* sp. isolated on ethene. *Environ. Sci. Technol.* **2001**, *35*, 4242–4251.
- (16) Singh, H.; Löffler, F. E.; Fathepure, B. Z. Aerobic biodegradation of vinyl chloride by a highly enriched mixed culture. *Biodegradation* **2004**, *15*, 197–204.
- (17) Fathepure, B. Z.; Elango, V. K.; Singh, H.; et al. Bioaugmentation potential of a vinyl chloride-assimilating *Mycobacterium* sp., isolated from a chloroethene-contaminated aquifer. *FEMS Microbiol Lett.* **2005**, *248*, 227–234.
- (18) Mattes, T. E.; Coleman, N. V.; Spain, J. C.; et al. Physiological and molecular genetic analyses of vinyl chloride and ethene biodegradation in *Nocardioides* sp. strain JS614. *Arch. Microbiol.* **2005**, *183*, 95–106.
- (19) Elango, V. K.; Liggenstoffer, A. S.; Fathepure, B. Z. Biodegradation of vinyl chloride and *cis*-dichloroethene by a *Ralstonia* sp. strain TRW-1. *Appl. Microbiol. Biotechnol.* **2006**, *72*, 1270–1275.
- (20) Coleman, N. V.; Spain, J. C. Epoxyalkane:coenzyme M transferase in the ethene and vinyl chloride biodegradation pathways of *Mycobacterium* strain JS60. *J. Bacteriol.* **2003**, *185*, 5536–5545.
- (21) Mattes, T. E.; Alexander, A. K.; Coleman, N. V. Aerobic biodegradation of the chloroethenes: pathways, enzymes, ecology, and evolution. *FEMS Microbiol Rev.* **2010**, *34*, 445–475.
- (22) He, J.; Ritalahti, K. M.; Yang, K.-L.; et al. Detoxification of vinyl chloride to ethene coupled to growth of an anaerobic bacterium. *Nature* **2003**, *424*, 62–65.
- (23) Cupples, A. M.; Spormann, A. M.; McCarty, P. L. Growth of a *Dehalococcoides*-like microorganism on vinyl chloride and *cis*-dichloroethene as electron acceptors as determined by competitive PCR. *Appl. Environ. Microbiol.* **2003**, *69*, 953–959.

- (24) Löffler, F. E.; Yan, J.; Ritalahti, K. M.; et al. *Dehalococcoides mccartyi* gen. nov., sp. nov., obligately organohalide-respiring anaerobic bacteria relevant to halogen cycling and bioremediation, belong to a novel bacterial class, *Dehalococcoidia* class nov., order *Dehalococcoidales* ord. nov. and family *Dehalococcoidaceae* fam. nov., within the phylum *Chloroflexi*. *Int. J. Syst. Evol.* **2013**, *63*, 625–635.
- (25) Yang, Y.; Higgins, S. A.; Yan, J.; et al. Grape pomace compost harbors organohalide-respiring *Dehalogenimonas* species with novel reductive dehalogenase genes. *ISME J.* **2017**, *11*, 2767–2780.
- (26) Chen, G.; Murdoch, F. K.; Xie, Y.; et al. Dehalogenation of chlorinated ethenes to ethene by a novel isolate, “*Candidatus Dehalogenimonas etheniformans*. *Appl. Environ. Microbiol.* **2022**, *88*, e00443–22.
- (27) Cui, Y.; Li, X.; Yan, J.; et al. *Dehalogenimonas etheniformans* sp. nov., a formate-oxidizing, organohalide-respiring bacterium isolated from grape pomace. *Int. J. Syst. Evol. Microbiol.* **2023**, *73*, No. 005881.
- (28) Staples, C. A.; Murphy, S. R.; McLaughlin, J. E.; et al. Determination of selected fate and aquatic toxicity characteristics of acrylic acid and a series of acrylic esters. *Chemosphere* **2000**, *40*, 29–38.
- (29) Wang, X.; Li, Y.; Wei, S.; et al. Toxicity evaluation of butyl acrylate on the photosynthetic pigments, chlorophyll fluorescence parameters, and oxygen evolution activity of *Phaeodactylum tricornutum* and *Platymonas subcordiformis*. *Environ. Sci. Pollut. Res.* **2021**, *28*, 60954–60967.
- (30) Osaki, Y.; Matsueda, T.; Nagase, M.; et al. The microbial degradability of aniline in river water and an attempt to use the level of the biodegradability as an indicator of water pollution. *Eisei Kagaku* **1991**, *37*, 411–417.
- (31) Gaszczak, A.; Kaleta, J.; Szczyrba, E.; et al. Kinetics of butyl acrylate biodegradation by selected strain of microorganisms. *Proc. ECOpole* **2013**, *7*, No. 061.
- (32) Wiedemeier, T. H.; Swanson, M. A.; Moutoux, D. E.; et al. *Technical Protocol for Evaluating Natural Attenuation of Chlorinated Solvents in Ground Water*. U.S. Environmental Protection Agency, Washington, D.C., 1998, EPA/600/R-98/128 (NTIS 99–130023).
- (33) Wiedemeier, T. H.; Rifai, H. S.; Newell, C. J.; et al. Evaluating Natural Attenuation. In *Natural Attenuation of Fuels and Chlorinated Solvents in the Subsurface*, 1999; pp 298–360.
- (34) Ritalahti, K. M.; Hatt, J. K.; Petrovskis, E.; et al. Groundwater sampling for nucleic acid biomarker analysis. In *Handbook of Hydrocarbon and Lipid Microbiology*, Timmis, K. N., Ed. Springer Berlin Heidelberg: Berlin, Heidelberg, 2010; pp 3407–3418.
- (35) Wilson, J. T.; Mills, J. C., IV; Wilson, B. H.; et al. Using qPCR assays to predict rates of cometabolism of TCE in aerobic groundwater. *Groundwater Monit. R.* **2019**, *39*, 53–63.
- (36) Taggart, D. M.; Clark, K. Lessons learned from 20 years of molecular biological tools in petroleum hydrocarbon remediation. *Remediation J.* **2021**, *31*, 83–95.
- (37) Lee, P. K. H.; Macbeth, T. W.; Sorenson, K. S.; et al. Quantifying genes and transcripts to assess the in situ physiology of “*Dehalococcoides*” spp. in a trichloroethene-contaminated groundwater site. *Appl. Environ. Microbiol.* **2008**, *74*, 2728–2739.
- (38) Cupples, A. M. Real-time PCR quantification of *Dehalococcoides* populations: Methods and applications. *J. Microbiol. Methods* **2008**, *72*, 1–11.
- (39) Ritalahti, K. M.; Hatt, J. K.; Lugmayr, V.; et al. Comparing on-site to off-site biomass collection for *Dehalococcoides* biomarker gene quantification to predict in situ chlorinated ethene detoxification potential. *Environ. Sci. Technol.* **2010**, *44*, 5127–5133.
- (40) Clark, K.; Taggart, D. M.; Baldwin, B. R.; et al. Normalized quantitative PCR measurements as predictors for ethene formation at sites impacted with chlorinated ethenes. *Environ. Sci. Technol.* **2018**, *52*, 13410–13420.
- (41) Jin, Y. O.; Mattes, T. E. A quantitative PCR assay for aerobic, vinyl chloride- and ethene-assimilating microorganisms in groundwater. *Environ. Sci. Technol.* **2010**, *44*, 9036–9041.
- (42) Liang, Y.; Liu, X.; Singletary, M. A.; et al. Relationships between the abundance and expression of functional genes from vinyl chloride (VC)-degrading bacteria and geochemical parameters at VC-contaminated sites. *Environ. Sci. Technol.* **2017**, *51*, 12164–12174.
- (43) Lu, X.; Wilson, J. T.; Campbell, D. H. Relationship between *Dehalococcoides* DNA in ground water and rates of reductive dechlorination at field scale. *Water Res.* **2006**, *40*, 3131–3140.
- (44) Lu, X.; Wilson, J. T.; Campbell, D. H. Comparison of an assay for *Dehalococcoides* DNA and a microcosm study in predicting reductive dechlorination of chlorinated ethenes in the field. *Environ. Pollut.* **2009**, *157*, 809–815.
- (45) Michalsen, M. M.; Kara Murdoch, F.; Löffler, F. E.; et al. Quantitative proteomics and quantitative PCR as predictors of *cis*-1,2-dichlorethane and vinyl chloride reductive dechlorination rates in bioaugmented aquifer microcosms. *ACS EST Engg* **2022**, *2*, 43–53.
- (46) Löffler, F. E.; Sanford, R. A.; Ritalahti, K. M. Enrichment, cultivation, and detection of reductively dechlorinating bacteria. *Methods Enzymol.* **2005**, *397*, 77–111.
- (47) Justicia-Leon, S. D.; Higgins, S.; Mack, E. E.; et al. Bioaugmentation with distinct *Dehalobacter* strains achieves chloroform detoxification in microcosms. *Environ. Sci. Technol.* **2014**, *48*, 1851–1858.
- (48) Ritalahti, K. M.; Cruz-García, C.; Padilla-Crespo, E.; et al. RNA extraction and cDNA analysis for quantitative assessment of biomarker transcripts in groundwater. In *Handbook of Hydrocarbon and Lipid Microbiology*, Timmis, K. N., Ed. Springer Berlin Heidelberg: Berlin, Heidelberg, 2010; pp 3671–3685.
- (49) Hatt, J. K.; Löffler, F. E. Quantitative real-time PCR (qPCR) detection chemistries affect enumeration of the *Dehalococcoides* 16S rRNA gene in groundwater. *J. Microbiol. Methods* **2012**, *88*, 263–270.
- (50) Hatt, J. K.; Ritalahti, K. M.; Ogles, D. M.; et al. Design and application of an internal amplification control to improve *Dehalococcoides mccartyi* 16S rRNA gene enumeration by qPCR. *Environ. Sci. Technol.* **2013**, *47*, 11131–11138.
- (51) Jugder, B.-E.; Ertan, H.; Bohl, S.; et al. Organohalide respiring bacteria and reductive dehalogenases: key tools in organohalide bioremediation. *Front Microbiol* **2016**, *7*, 249.
- (52) Yan, J.; Wang, J.; Villalobos Solis, M. I.; et al. Respiratory vinyl chloride reductive dechlorination to ethene in *TceA*-expressing *Dehalococcoides mccartyi*. *Environ. Sci. Technol.* **2021**, *55*, 4831–4841.
- (53) Jin, Y. O.; Mattes, T. E. Assessment and modification of degenerate qPCR primers that amplify functional genes from etheneotrophs and vinyl chloride-assimilators. *Lett. Appl. Microbiol.* **2011**, *53*, 576–580.
- (54) Friedrich, M. W. Phylogenetic analysis reveals multiple lateral transfers of adenosine-5'-phosphosulfate reductase genes among sulfate-reducing microorganisms. *J. Bacteriol.* **2002**, *184*, 278–289.
- (55) Suzuki, M. T.; Taylor, L. T.; DeLong, E. F. Quantitative analysis of small-subunit rRNA genes in mixed microbial populations via 5'-nuclease assays. *Appl. Environ. Microbiol.* **2000**, *66*, 4605–4614.
- (56) Ritalahti, K. M.; Amos, B. K.; Sung, Y.; et al. Quantitative PCR targeting 16S rRNA and reductive dehalogenase genes simultaneously monitors multiple *Dehalococcoides* strains. *Appl. Environ. Microbiol.* **2006**, *72*, 2765–2774.
- (57) Borchardt, M. A.; Boehm, A. B.; Salit, M.; et al. The Environmental microbiology minimum information (EMMI) guidelines: qPCR and dPCR Quality and reporting for environmental microbiology. *Environ. Sci. Technol.* **2021**, *55*, 10210–10223.
- (58) Klindworth, A.; Pruesse, E.; Schweer, T.; et al. Evaluation of general 16S ribosomal RNA gene PCR primers for classical and next-generation sequencing-based diversity studies. *Nucleic Acids Res.* **2013**, *41*, No. e1.
- (59) Thijs, S.; Op De Beeck, M.; Beckers, B.; et al. Comparative evaluation of four bacteria-specific primer pairs for 16S rRNA gene surveys. *Front Microbiol* **2017**, *8*, 494.
- (60) Bolyen, E.; Rideout, J. R.; Dillon, M. R.; et al. Reproducible, interactive, scalable and extensible microbiome data science using QIIME 2. *Nat. Biotechnol.* **2019**, *37*, 852–857.
- (61) Callahan, B. J.; McMurdie, P. J.; Rosen, M. J.; et al. DADA2: High-resolution sample inference from Illumina amplicon data. *Nat. Methods* **2016**, *13*, 581–583.

- (62) Quast, C.; Pruesse, E.; Yilmaz, P.; et al. The SILVA ribosomal RNA gene database project: improved data processing and web-based tools. *Nucleic Acids Res.* **2012**, *41*, D590–D596.
- (63) Yilmaz, P.; Parfrey, L. W.; Yarza, P.; et al. The SILVA and “All-species Living Tree Project (LTP)” taxonomic frameworks. *Nucleic Acids Res.* **2014**, *42*, D643–D648.
- (64) McMurdie, P. J.; Holmes, S. phyloseq: An R package for reproducible interactive analysis and graphics of microbiome census data. *PLoS One* **2013**, *8*, No. e61217.
- (65) Friendly, M.; Monette, G.; Fox, J. Elliptical insights: understanding statistical methods through elliptical geometry. *Stat Sci.* **2013**, *28*, 1–39.
- (66) Oksanen, J.; Kindt, R.; Legendre, P.; et al. The Vegan Package. *Commun. Ecol. Package* **2007**, *10*, 719.
- (67) Chen, G.; Jiang, N.; Villalobos Solis, M. I.; et al. Anaerobic microbial metabolism of dichloroacetate. *mBio* **2021**, *12*, e00537–21.
- (68) Chen, G.; Fisch, A. R.; Gibson, C. M.; et al. Mineralization versus fermentation: evidence for two distinct anaerobic bacterial degradation pathways for dichloromethane. *ISME J.* **2020**, *14*, 959–970.
- (69) Cápiro, N. L.; Wang, Y.; Hatt, J. K.; et al. Distribution of organohalide-respiring bacteria between solid and aqueous phases. *Environ. Sci. Technol.* **2014**, *48*, 10878–10887.
- (70) Rosolina, S. M.; Carpenter, T. S.; Xue, Z.-L. Bismuth-based, disposable sensor for the detection of hydrogen sulfide gas. *Anal. Chem.* **2016**, *88*, 1553–1558.
- (71) Fullerton, H.; Crawford, M.; Bakken, A.; et al. Anaerobic oxidation of ethene coupled to sulfate reduction in microcosms and enrichment cultures. *Environ. Sci. Technol.* **2013**, *47*, 12374–12381.
- (72) Coleman, N. V.; Mattes, T. E.; Gossett, J. M.; et al. Phylogenetic and kinetic diversity of aerobic vinyl chloride-assimilating bacteria from contaminated Sites. *Appl. Environ. Microbiol.* **2002**, *68*, 6162–6171.
- (73) Liu, X.; Wu, Y.; Wilson, F. P.; et al. Integrated methodological approach reveals microbial diversity and functions in aerobic groundwater microcosms adapted to vinyl chloride. *FEMS Microbiol. Ecol.* **2018**, *94*, fwy124.
- (74) Jin, Y. O.; Mattes, T. E. Adaptation of aerobic, ethene-assimilating *Mycobacterium* strains to vinyl chloride as a growth substrate. *Environ. Sci. Technol.* **2008**, *42*, 4784–4789.
- (75) Richards, P. M.; Ewald, J. M.; Zhao, W.; et al. Natural biodegradation of vinyl chloride and *cis*-dichloroethene in aerobic and suboxic conditions. *Environ. Sci. Pollut. Res.* **2022**, *29*, 56154–56167.
- (76) Freedman, D. L.; Danko, A. S.; Verce, M. F. Substrate interactions during aerobic biodegradation of methane, ethene, vinyl chloride and 1,2-dichloroethenes. *Water Sci. Technol.* **2001**, *43*, 333–40.
- (77) Findlay, M.; Smoler, D. F.; Fogel, S.; et al. Aerobic vinyl chloride metabolism in groundwater microcosms by methanotrophic and etheneotrophic bacteria. *Environ. Sci. Technol.* **2016**, *50*, 3617–3625.
- (78) Ghodke, V. M.; Punekar, N. S. Environmental role of aromatic carboxylesterases. *Environ. Microbiol.* **2022**, *24*, 2657–2668.
- (79) Lai, J.; Huang, H.; Lin, M.; et al. Enzyme catalyzes ester bond synthesis and hydrolysis: The key step for sustainable usage of plastics. *Front Microbiol* **2023**, *13*, No. 1113705.
- (80) Schink, B. Energetics of syntrophic cooperation in methanogenic degradation. *Microbiol. Mol. Biol. Rev.* **1997**, *61*, 262–280.
- (81) Ladd, J. N.; Walker, D. J. The fermentation of lactate and acrylate by the rumen microorganism. *Biochem. J.* **1959**, *71*, 364–373.
- (82) Akedo, M.; Cooney, C. L.; Sinskey, A. J. Direct demonstration of lactate–acrylate interconversion in *Clostridium Propionicum*. *Nat. Biotechnol.* **1983**, *1*, 791–794.
- (83) Janssen, P. H. Isolation of *Clostridium propionicum* strain 19acry3 and further characteristics of the species. *Arch. Microbiol.* **1991**, *155*, 566–571.
- (84) Qu, M.; Bhattacharya, S. K. Degradation and toxic effects of acrylic acid on anaerobic systems. *J. Environ. Eng.* **1996**, *122*, 749–756.
- (85) He, J.; Sung, Y.; Dollhopf, M. E.; et al. Acetate versus hydrogen as direct electron donors to stimulate the microbial reductive dechlorination process at chloroethene-contaminated sites. *Environ. Sci. Technol.* **2002**, *36*, 3945–3952.
- (86) Chen, G.; Yang, Y.; Yan, J.; et al. Metabolite cross-feeding enables concomitant catabolism of chlorinated methanes and chlorinated ethenes in synthetic microbial assemblies. *ISME J.* **2024**, *18*, No. wrae090.
- (87) GlobalData Plc. <https://www.globaldata.com/>.
- (88) Zhang, M.; Buekens, A.; Jiang, X.; et al. Dioxins and polyvinylchloride in combustion and fires. *Waste Manag. Res.* **2015**, *33*, 630–643.
- (89) Oladeji, O.; Saitas, M.; Mustapha, T.; et al. Air pollutant patterns and human health risk following the East Palestine, Ohio, train derailment. *Environ. Sci. Technol. Lett.* **2023**, *10*, 680–685.
- (90) Sloop, J. T.; Chao, A.; Gundersen, J.; et al. Demonstrating the use of non-targeted analysis for identification of unknown chemicals in rapid response scenarios. *Environ. Sci. Technol.* **2023**, *57*, 3075.
- (91) NewsNation. *East Palestine dioxins thousands of times higher than control*: Scientist. <https://www.newsnationnow.com/us-news/midwest/ohio-train-derailment/extreme-levels-cancer-chemicals-east-palestine-soil/#text=On%20May%2015%20independent%20testing,Street%20%20Smith%20old%20NewsNation>.
- (92) Runwal, P. Vent and burn ‘unnecessary’ in East Palestine, safety board finds. *C&EN (Chemical & Engineering News)*, **2024**, *102* 14, <https://cen.acs.org/environment/Decision-vent-burn-unnecessary-National/102/i20>.
- (93) Haynes, E. N.; Eskenazi, B.; Hilbert, T. J.; et al. Serum dioxin levels in a subset of participants of the East Palestine, Ohio train derailment health tracking study. *Environ. Sci. Technol. Lett.* **2024**, *11*, 673–678.
- (94) Hofstetter, T. B.; Bakkour, R.; Buchner, D.; et al. Perspectives of compound-specific isotope analysis of organic contaminants for assessing environmental fate and managing chemical pollution. *Nat. Water* **2024**, *2*, 14–30.